

## **A Parameter-Insensitive False Alarm Rate Detection Processor**

David M. Drumheller and Henry Lew

DSTO-TR-1153

**DISTRIBUTION STATEMENT A**  
Approved for Public Release  
Distribution Unlimited

# A Parameter-Insensitive False Alarm Rate Detection Processor

*David M. Drumheller and Henry Lew*

Maritime Operations Division  
Aeronautical and Maritime Research Laboratory

DSTO-TR-1153

## ABSTRACT

In active sonar systems, detection is the process of deciding if a target echo is present in a return. This is often accomplished by an operator who examines the sonar receiver output and decides if any portion of it is larger than the expected response due to reverberation. Detection may also be accomplished automatically using a processor that sets a threshold based on a sampling of the receiver output. In this report, a detection processor developed under the task NAV 99/027 is presented for use in active sonar systems that process returns incoherently. The statistics of the receiver output of such a system follows the two-parameter gamma probability density function (PDF). Consequently, the detection processor computes the detection threshold as a non-linear function of the ratio of two ranked values of the receiver output. The result is a detection processor that exhibits a false alarm probability that is bounded within ten percent of a design value regardless of the values of the gamma PDF parameters.

20010809076

APPROVED FOR PUBLIC RELEASE



AQ F01-11-2214

*Published by*

*DSTO Aeronautical and Maritime Research Laboratory  
506 Lorimer St,  
Fishermans Bend, Victoria, Australia 3207*

*Telephone: (03) 9626 7000  
Facsimile: (03) 9626 7999*

*© Commonwealth of Australia 2001  
AR No. AR-011-869  
June, 2001*

**APPROVED FOR PUBLIC RELEASE**

## A Parameter-Insensitive False Alarm Rate Detection Processor

### EXECUTIVE SUMMARY

In active sonar systems, detection is the process of deciding if a target echo is present in a sonar return. This is often accomplished by an operator who examines the sonar receiver output and decides if any portion of the output is larger than the expected response due to reverberation. If so, then a target is declared to be present at the range and bearing associated with the "peak" in the receiver output.

When ping cycles are short or alert periods are long, operators may become unreliable and falsely dismiss echoes that indicate the presence of a target. In light of this, it is desirable to employ algorithms that automatically detect the presence of a possible target, thus freeing the operator for other tasks, including the further processing of a return to classify the exact nature of a detected echo. Commonly, such processors are designed to maintain a constant probability of false alarm per display resolution cell, which is usually between  $10^{-6}$  and  $10^{-3}$ . Such processors use samples of the receiver output to implicitly estimate the parameters of its statistical model and appropriately set a detection threshold. Any portion of the receiver output exceeding this threshold is flagged as a possible target.

In this report, a detection processor developed under the Navy sponsored task NAV 99/027 is presented for use in active sonar systems that process returns incoherently. The statistics of the receiver output of such a system follows the two-parameter gamma probability density function (PDF). Consequently, the detection processor computes the detection threshold as a non-linear function of the ratio of two ranked values of the receiver output samples. The result is a detection processor that exhibits a false alarm probability that is bounded within some range around its design value regardless of the true values of the gamma PDF parameters. Hence, the processor is said to exhibit a "parameter-insensitive" false alarm rate.

This report documents a technique for deriving "parameter-insensitive-false-alarm-rate" (PIFAR) detection processors. A design example is presented. The coefficients of the polynomial approximations to the detection processor non-linearity, which are needed to implement the processor, are tabulated in Appendix A.



## Contents

<b>Glossary</b>	<b>vii</b>
<b>1</b> <b>Introduction</b>	<b>1</b>
<b>2</b> <b>CFAR Processing</b>	<b>1</b>
<b>3</b> <b>PIFAR Processing</b>	<b>3</b>
<b>4</b> <b>PIFAR Detection Processor Design</b>	<b>5</b>
<b>5</b> <b>Design Example</b>	<b>6</b>
<b>6</b> <b>Performance</b>	<b>7</b>
<b>7</b> <b>Conclusion</b>	<b>12</b>
<b>References</b>	<b>13</b>

## Appendices

<b>A</b> <b>Polynomial Approximations to PIFAR Detector Non-Linearities</b>	<b>14</b>
---	-----------

## Figures

<b>1</b> The generic CFAR detection processor architecture. . . . .	<b>2</b>
<b>2</b> The PIFAR detection processor architecture. . . . .	<b>4</b>
<b>3</b> The initial and final curves of the probability of false alarm as a function of the shape for the design example of a PIFAR processor for $N = 60$ with $i = 15$ and $j = 45$ . . . . .	<b>7</b>
<b>4</b> The initial and final curves for the PIFAR processor non-linearity for the design example for $N = 60$ with $i = 15$ and $j = 45$ . . . . .	<b>8</b>
<b>5</b> Depiction of the SNR loss between and ideal processor and a CFAR detection processor. SNR loss is commonly defined as the difference in SNR between the ROC curves for a specified probability of detection, which in this case is 0.5. . . . .	<b>9</b>
<b>6</b> The average SNR loss (ASNRL) in dB as a function of the number of data cells ( $N$ ) for PIFAR processors with a design probability of false alarm of $10^{-3}$ . For these processors, $N = 4K$ , $I = K$ and $j = 3K$ where $K$ is an integer. . . . .	<b>10</b>

7 The average SNR loss (ASNRL) in dB as a function of the number of data cells ( $N$ ) for PIFAR processors with a design probability of false alarm of  $10^{-4}$ . For these processors,  $N = 4K$ ,  $I = K$  and  $j = 3K$  where  $K$  is an integer. 10

8 The average SNR loss (ASNRL) in dB as a function of the number of data cells ( $N$ ) for PIFAR processors with a design probability of false alarm of  $10^{-5}$ . For these processors,  $N = 4K$ ,  $I = K$  and  $j = 3K$  where  $K$  is an integer. 11

9 The average SNR loss (ASNRL) in dB as a function of the number of data cells ( $N$ ) for PIFAR processors with a design probability of false alarm of  $10^{-6}$ . For these processors,  $N = 4K$ ,  $I = K$  and  $j = 3K$  where  $K$  is an integer. 11

## Tables

A1	Argument limits and bounds for the eighth-order polynomial approximations to PIFAR detection processor non-linearities, where $N$ is the number of data cells and $i$ and $j$ are the rank orders. . . . .	15
A2	Coefficients $b_5$ through $b_8$ for the eighth-order polynomial approximations to PIFAR detection processor non-linearities, where $N$ is the number of data cells and $i$ and $j$ are the rank orders. . . . .	16
A3	Coefficients $b_1$ through $b_4$ for the eighth-order polynomial approximations to PIFAR detection processor non-linearities, where $N$ is the number of data cells and $i$ and $j$ are the rank orders. . . . .	17
A4	Coefficient $b_0$ (additive constant) for the eighth-order polynomial approximations to PIFAR detection processor non-linearities, where $N$ is the number of data cells and $i$ and $j$ are the rank orders. . . . .	18

## Glossary

**ADT** average detection threshold

**ASNRL** average signal-to-noise ratio loss

**CDF** cumulative distribution function

**CFAR** constant false alarm rate

**OS-CFAR** order statistic constant false alarm rate

**PDF** probability density function

**PIFAR** parameter-insensitive false alarm rate

**SNR** signal-to-noise ratio

**SNRL** signal-to-noise ratio loss

**TM-CFAR** trimmed mean constant false alarm rate



## 1 Introduction

All active sonar systems process echoes to produce an image of the tactical area surrounding the source and the processing platform. In the case of systems that incoherently process echoes, the signals from the receiver array are often beamformed and then passed through one or more bandpass filters to yield a range-bearing or bearing-Doppler map. These maps are examined by an operator whose principal task is to decide if any feature of the map is indicative of a target. Generally speaking, this amounts to examining any peak ("hot spot") and declaring it a potential target when its value is significantly higher than the average level of the surrounding area in the map.

This process of target detection can be automated, thereby reducing the operator task load. This requires a statistical model for the data in the map from which an appropriate detection processor may be found. The common class of processors used to accomplish automatic detection is referred to as "constant-false-alarm-rate" (CFAR) detection processors.

To date, nearly every CFAR detection processor reported in the literature is based on a statistical model that is dependent upon a single, unknown parameter that is proportional to the expected magnitude or power of the data. In our work, we have found that a two-parameter model may be more appropriate, so that none of the algorithms reported in the literature can be used<sup>1</sup>. This additional parameter does not describe the power of the data, but the general shape of its probability density function (PDF).

The class of detection processors presented in this report have been developed for use in an incoherent sonar system whose receiver output (the range-bearing map) follows a gamma PDF, a statistical model that is described by a "scale parameter," which is proportional to the power, and a "shape parameter." In effect, the processor estimates the power of the data from which a detection threshold is derived, the threshold being insensitive to the value of the shape parameter.

The remainder of this report begins with a general review of the conventional CFAR approach to detection. This follows with a description of the new approach where processors are designed to be insensitive to the value of the shape parameter of the statistical model of the sonar receiver output. A recursive technique for deriving these "parameter-insensitive" detection processors is then presented. The report concludes with an analysis of their performance.

## 2 CFAR Processing

Consider the case of a sonar receiver that produces a conventional "B-scan," which displays the return echo amplitude or power as a function of range only. Because the receiver possesses a fixed range resolution, which is related to the echo's time length and bandwidth, the receiver output can be divided into "bins" or "cells" of equal width in

---

<sup>1</sup>CFAR processors have been designed for two-parameter statistical models but with the assumption that one of the parameters is known *a priori*, thus effectively reducing the problem to that of the one-parameter case. An exception to this is the work of Refs. [1] and [2], although their technique appears to be specific to the Weibull distribution.

range. Values of the output can be sampled at the centre of each cell. Detection amounts to comparing the receiver output samples to a threshold,  $\gamma$ , and declaring a target present if any of the values exceeds it.

In sonar systems, it is often the case that the statistical nature of receiver output is constant—a single PDF models all the data—but the power (expected square value) of the output is different at each point in range. This labours the detection processor with the additional task of estimating the PDF parameter that relates directly to the power. The structure of a detection processor for performing these tasks is shown in Fig. 1. It draws samples from the “data cells,”  $X_1, \dots, X_N$ , that are used to compute a threshold to which the “test cell” value,  $T$ , is compared. This threshold is expressed as a product of the estimate of the data’s expected power,  $Y$ , and an appropriately chosen “multiplier,”  $\beta$ . Moreover, the threshold should be set so as not to allow too many detections to occur, thereby overloading the operator. Therefore, the probability of a false alarm—the probability of a single receiver output exceeding the threshold when no target is present—is usually quite small in practice. Typical values range from  $10^{-6}$  to  $10^{-3}$ . If the cumulative distribution function (CDF) of the test cell sample,  $F_T(t)$ , is known (no target assumed to be present), then the probability of false alarm is given by

$$P_{fa}(\beta) = \int_0^\infty [1 - F_T(\beta y)] f_Y(y) dy, \quad (1)$$

where  $f_Y(y)$  is the PDF of the data’s expected power. In most cases, there will be no analytic form for the multiplier, so a numerical technique, such as Newton’s method, must be employed to find it.

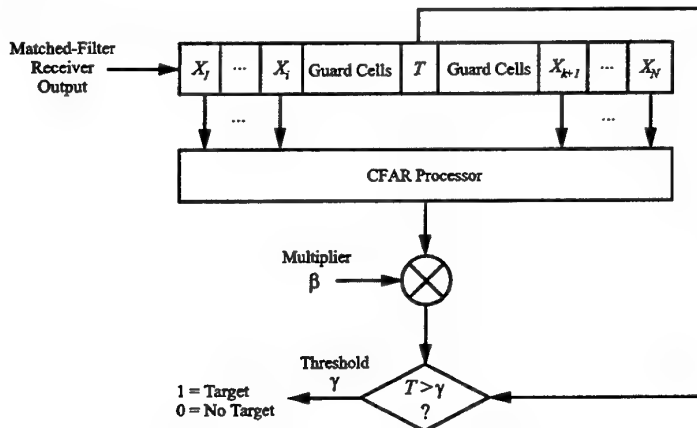


Figure 1: The generic CFAR detection processor architecture.

Under the assumptions stated above, the resulting detection processor exhibits a constant false alarm probability. Thus, such processors are referred to as “constant-false-alarm-rate” (CFAR) detection processors. A number of techniques have been reported that yield the CFAR detection processor as defined by Eq. (1) for several families of statistical models, each having their own advantages and disadvantages. For example, the values of the data cells can be averaged to yield an estimate of the power, which is known as “cell-averaging CFAR” (CA-CFAR) [3]. This technique provides a low-variance estimate of the power, but can yield high threshold levels if a target return is present in one

of the data cells. This may be corrected by using a trimmed-mean technique (TM-CFAR) [4] or order statistics (OS-CFAR) [5, 6] to discard the non-representative data cell values, thus rendering a robust threshold.

### 3 PIFAR Processing

The detection processor presented in this report is developed for an incoherent sonar system. A common operation in the incoherent detection of signals is quadratic detection, which consists of the summation of the squares of many independent samples. In effect the detector is measuring the energy of the echo returns. If the samples follow a zero mean Gaussian random process then the detector output will be gamma distributed (with a shape parameter equal to half the total number of samples in the sum). Here, we assume that the detector output in the absence of a target follows a gamma distribution with no restrictions on its shape parameter. The form of the gamma PDF is given by

$$f_X(x) = \frac{1}{b\Gamma(c)} \left(\frac{x}{b}\right)^{c-1} \exp\left(-\frac{x}{b}\right), \quad (2)$$

where  $X$  a random variable representing the energy of the receiver response to ocean reverberation, and  $b$  and  $c$  are the scale and shape parameters of the distribution, respectively.

Because the gamma PDF is defined by two parameters, the threshold may be set using estimates of both parameters. In this case, two statistics based on the data cells must be used, and so we propose the following generalisation of the false alarm probability defined in Eq. (1):

$$P_{fa}(\beta) = \int_0^\infty \int_0^\infty [1 - F_T(\beta(x, y))] f_{X,Y}(x, y) dx dy. \quad (3)$$

Here,  $X$  and  $Y$  are statistics that in some way measure the shape and scale parameters respectively and  $f_{X,Y}(x, y)$  is their joint PDF. We need only choose the functional relationships between these statistics and the data cells so that the PDF in the integrand can be evaluated. Furthermore, we should choose these statistics so that the resulting detection processor is insensitive to target returns falling within the data cells.

In light of these requirements, we chose  $X$  and  $Y$  to be order statistics because such detection processors are robust against multiple target returns appearing in the data cells. Thus, if  $X_1, \dots, X_N$  are the original values of the data cells, let  $Y_1, \dots, Y_N$  be these values after ordering in ascending magnitude (i.e.,  $Y_i \leq Y_{i+1}$ ). By using  $Y_i < Y_j$ , let

$$Z = \ln(Y_j/Y_i), \quad (4)$$

which is a statistic that is insensitive to any scaling<sup>2</sup>. Next, choose  $X = Y_i$  and  $Y = Y_j$ , the larger of the two order statistics. In this case, Eq. (3) becomes

$$P_{fa}(\beta) = \int_0^\infty \int_0^\infty [1 - F_T(\beta(z, y))] f_{Z,Y}(z, y) dz dy, \quad (5)$$

<sup>2</sup>This is easy to see, for if  $Y_i \rightarrow \alpha Y_i$  and  $Y_j \rightarrow \alpha Y_j$  for some constant  $\alpha$ , the statistic  $Z$  is unchanged.

where  $f_{X,Y}(x, y)$  is related to  $f_{Z,Y}(z, y)$  via a transformation of random variables such that

$$f_{Z,Y}(z, y) = ye^{-z} f_{X,Y}(ye^{-z}, y). \quad (6)$$

In turn, the joint PDF for  $X$  and  $Y$  is just the joint PDF for a pair of order statistics, which is given by

$$\begin{aligned} f_{X,Y}(x, y) = & \frac{N!}{(i-1)!(j-i-1)!(N-j)!} [F_{Y_i}(x)]^{i-1} f_{Y_i}(x) \\ & \times [F_{Y_j}(y) - F_{Y_i}(x)]^{j-i-1} f_{Y_j}(y) \\ & \times [1 - F_{Y_j}(y)]^{N-j} u(y - x), \end{aligned} \quad (7)$$

where  $u(\cdot)$  denotes the unit step function [7] and  $f_X(\cdot)$  and  $F_X(\cdot)$  are the PDF and CDF of the values of each data cell, respectively. Thus, through substitution, the integrand of Eq. (5) can be evaluated if the PDF and CDF for each data cell are known. The structure of the PIFAR processes as described by Eqs. (5) through (7) is shown in Fig. 2.

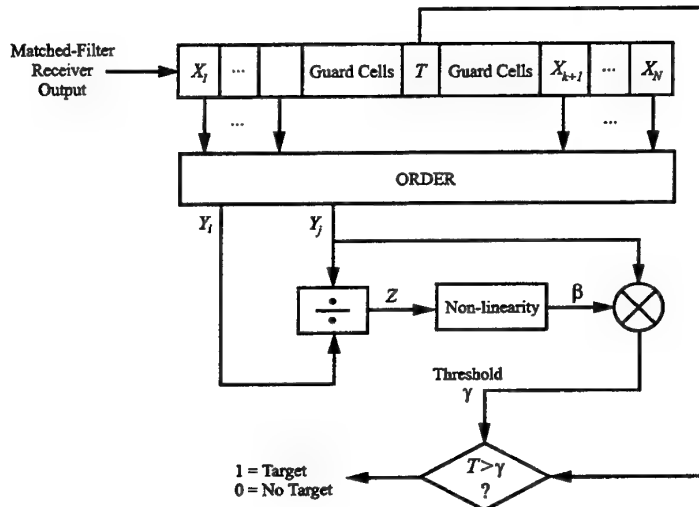


Figure 2: The PIFAR detection processor architecture.

The values of  $i$  and  $j$ , the rank orders, are arbitrary, although some thought reveals what could be considered “best choices” in light of some trade offs. Roughly speaking, the shape parameter provides a measure of the “width” of the PDF,  $f_X(x)$ . Consequently, it is reasonable to expect that by choosing two order statistics that are significantly different in rank, a PIFAR detection processor’s performance would be insensitive to the shape parameter. It follows that  $i = 1$  and  $j = N$  would be the best choices. On the other hand, CFAR algorithms based on order statistics are known to be insensitive to target or false target responses appearing in the data cells, particularly if the median value of the ranked cell values is used. This would imply that  $i$  and  $j$  should be equal to the integer nearest or equal to  $N/2$ . A compromise between these two competing properties can be made by choosing  $i = K$  and  $j = 3K$  with  $K$  equal to the integer closest to  $N/4$ . A similar observation regarding the choice of rank orders have been made for order statistic

CFAR detection processors designed for detecting targets in radar clutter that follows the two-parameter Weibull PDF [2].

Examination of Eq. (5) reveals that designing a detection processor amounts to finding a function,  $\beta(\cdot)$ , that yields an integral that is equal to  $P_{fa}$  regardless of the shape parameter of the statistical model for the data cells. Unfortunately, there does not appear to be a way to solve this integral equation in general. Nevertheless, there is a way to recursively find a function,  $\beta(\cdot)$ , such that false alarm probability is *insensitive* to the shape parameter. Thus, a detection processor based on such a nonlinearity yields a “parameter-insensitive false alarm rate” (PIFAR), and so it is called a “PIFAR detection processor.”

## 4 PIFAR Detection Processor Design

The integral equation in Eq. (5) cannot be solved in closed form. Consequently, a recursive technique for solving the integral equation was developed and is outlined below.

Starting with an initial guess for  $\beta(\cdot)$ , the multiplier is repeatedly perturbed until the resulting  $P_{fa}$  is sufficiently close to a constant design value,  $\hat{P}_{fa}$ , over the range of shape parameters likely to be encountered in practice. A technique for perturbing the multiplier was deduced by examining the first variation of the integral expressing the  $P_{fa}$  as a functional of the multiplier, which is given by

$$\delta P_{fa}(\beta, \eta) = \lim_{\epsilon \rightarrow 0} \frac{d}{d\epsilon} P_{fa}(\beta + \epsilon\eta) = - \int_0^\infty I(z|\beta, b, c) \eta(z) dz, \quad (8)$$

where

$$I(z|\beta, b, c) = \frac{1}{\Gamma(c)} \int_0^\infty \beta^{c-1}(z) \left(\frac{y}{b}\right)^c \exp\left(-\frac{\beta(z)y}{b}\right) f_{Z,Y}(z, y) dy. \quad (9)$$

Though expressed as a double integral, the first variation suggests how a perturbation to the multiplier may be chosen. First, if any perturbation of the multiplier is proportional to the integral in Eq. (9) it will surely change the value of  $P_{fa}$ . Second, for any value of  $c$ , the sign of the perturbation should be proportional to sign of the difference  $P_{fa}(c) - \hat{P}_{fa}$ . Third, any perturbation should be proportional to the relative difference in size, which may be expressed logarithmically. These observations justifies the following heuristic choice for the perturbation:

$$\delta\beta(z) = \alpha \sum_{m=1}^M \frac{\operatorname{sgn}(P_{fa}(c_m) - \hat{P}_{fa})}{(c_m + 1) \max_z I(z|\beta, b, c_m)} \left| \ln \left( \frac{P_{fa}(c_m)}{\hat{P}_{fa}} \right) \right| I(z|\beta, b, c_m). \quad (10)$$

The summation over a range of shape parameter values results in a non-linearity that yields a processor that is insensitive to the shape parameter. With Eq. (10), the multiplier can be found by first choosing an initial functional form for  $\beta(\cdot)$  and then repeatedly perturbing it using Eq. (10). In practice, a workable choice for the values of the shape parameter in Eq. (10) is

$$c_m = c_{\min} + (c_{\max} - c_{\min})(m - 1)/M \quad \text{for } m = 1, \dots, M, \quad (11)$$

with  $c_{\min} = 5$ ,  $c_{\max} = 40$  and  $M = 35$ . Furthermore,  $\alpha = 0.25$  was empirically found to be a good choice.

The initial choice of  $\beta(z)$  was a piecewise linear interpolation between the values of the multiplier found by solving Eq. (1) for each  $c_m$  and associating it with the average value of  $Z$  found by numerically evaluating

$$\bar{Z} = \int_0^\infty \int_0^\infty z f_{Z,Y}(z, y) dz dy. \quad (12)$$

Because in practice it is impossible to optimise the detection processor for all possible values of the shape parameter, hard limits are established on the range of possible values for the multiplier. Written as  $\beta_L$  and  $\beta_H$  to denote the lowest and highest values for the multiplier, these limits are used when  $Z$  either falls below  $\beta_L$  or exceeds  $\beta_H$ . The values of  $\beta_L$  and  $\beta_H$  are initially set equal to the expected values of  $Z$  that are computed for  $c_1$  and  $c_M$ .

It can be seen that as the shape parameter decreases, the tail of the gamma probability density function becomes broader, thus implying that the detection threshold should increase with respect to the mean. Accordingly, it is reasonable to expect that the mapping  $\beta(\cdot)$  is an increasing monotonic function. If the mapping is perturbed by blindly applying Eq. (10), there is risk of causing it to become non-increasing. This was remedied by adjusting the array holding the samples of the multiplier. Starting from the middle element of the array, the samples were made to increase after each perturbation by ensuring that by stepping from sample to sample in the forward (backward) direction that each sample was made to be at least as large as (no larger than) the previous sample.

After the recursive procedure outlined has been employed, the samples of the non-linearity may be stored for use in a real-world detection processor, though this was found to be unnecessary. A more compact way of storing the function is to fit it to a polynomial in the interval  $[z_L, z_H]$ . This may be accomplished using a least squares approach subject to the constraint that the polynomial matches the value of the non-linearity at  $z_L$  and  $z_H$ .

PIFAR processor non-linearities were computed for  $i = K$ ,  $j = 3K$  and  $K$  equal to 11, 13, 15, 17, 19, 21, 23, 25 and 27. These non-linearities are well approximated by eighth-order polynomials, the coefficients of which are listed in Appendix A.

## 5 Design Example

Consider designing a PIFAR detection processor for  $P_{fa} = 10^{-4}$  with  $N = 60$ ,  $i = 60/4 = 15$  and  $j = 3i = 45$ .

Application of the algorithm for finding the non-linearity,  $\beta(\cdot)$ , outlined in the previous section requires several integrals to be numerically evaluated. This was done by converting them into rectangular sums derived from uniformly sampling an interval or region. In the case of Eq. (5), the integrands were computed over a region centred approximately at the peak of the integrand that contained at least 99% of the area under the surface of the integrand. The area was sampled as a uniform grid with 30 samples along the  $y$  axis and 35 samples along the  $z$  axis. This grid was also used to evaluate the integrals in Eqs. (9) and (12).

Of course, the non-linearity,  $\beta(\cdot)$ , must also be discretised and this was done using a step size that is 1/4-th the size of the smallest step size for  $z$  that is used to evaluate the

double integral in Eq. (5). This is the same step size used to discretise the perturbations defined by Eq. (10). When the discretised version of  $\beta(\cdot)$  is used to compute the integrand of Eq. (5), the values required are found through interpolation.

The discrete values of the shape parameter used to compute the perturbation of  $\beta(\cdot)$  described by Eq. (10) were chosen using Eq. (11) with  $c_{min} = 5$ ,  $c_{max} = 40$  and  $M = 35$ . For all of the polynomial approximations to the non-linearities reported in Appendix A,  $c_{min} = 2$  and  $c_{max} = 40$ . For the parameter,  $\alpha$ , used to scale the perturbations, a value of 0.5 was used.

Using the step sizes and various parameter values described above, the non-linear multiplier was computed using 15 iterations according the prescription outlined in the previous section. Fig. 3 shows the value of  $P_{fa}$  as a function of shape parameter for the initial and final (optimised) non-linearity. The figure reveals that for  $5 < c < 30$ , the final non-linearity is within 10% of the objective value of  $P_{fa} = 10^{-4}$ . Fig. 4 shows the initial and final non-linearities. The final non-linearity was fitted to an 8-th order polynomial between  $z_L$  and  $z_H$ . The values of these bounds and the coefficients of this polynomial are listed in tables in Appendix A. The difference between  $\beta(\cdot)$  and its polynomial fit is quite close, and would not be clearly observable if plotted in Fig. 4. It was found that the polynomial fit actually reduced the error between the design value,  $\hat{P}_{fa}$ , and its actual value shown in Fig. 3 for  $20 < c < 35$ , although this would also not be clearly visible in the figure.

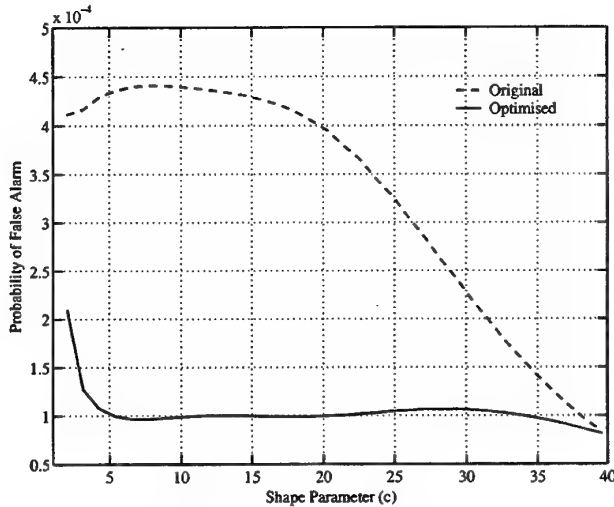


Figure 3: The initial and final curves of the probability of false alarm as a function of the shape for the design example of a PIFAR processor for  $N = 60$  with  $i = 15$  and  $j = 45$ .

## 6 Performance

Performance of a detector is most commonly expressed by fixing the probability of false alarm and then listing the probability of detection for a range of SNRs. This is possible if a statistical model is available that describes the behaviour of the receiver output when a

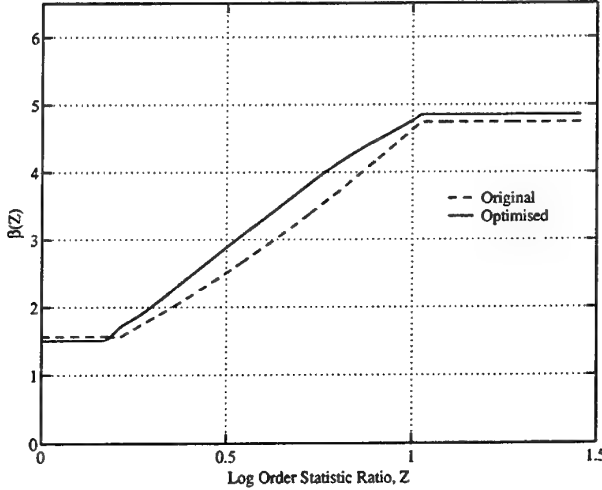


Figure 4: The initial and final curves for the PIFAR processor non-linearity for the design example for  $N = 60$  with  $i = 15$  and  $j = 45$ .

target return is present in the received echo. Such a model is often specific to the target, so for this analysis, which is to be generic, it is unreasonable to assume any specific model. The next best thing is to simply set the false alarm rate (based on an analysis of the system's operational use), use it to set the per-cell false alarm probability and accept the resulting probability of detection.

Since the PIFAR detector effectively estimates the statistical parameters of the environment and sets the threshold based on these estimates, it is reasonable to expect some loss of performance with respect to the ability to detect the target. Indeed, it is well known that CFAR detectors always exhibit detection probabilities that are lower than those exhibited by detection processors that clairvoyantly know the exact values of the statistical parameters of the environment. The difference between the detection probabilities of the two detectors is expressed by the "SNR loss," defined to be the increase in SNR required for the PIFAR detection processor to exhibit the same referenced  $P_d$  as the clairvoyant detection processor. This is illustrated in Fig. 5 where the referenced  $P_d$  is 0.5, the most common reference value quoted in the literature.

The SNR loss is also dependent upon the target characteristics, but fortunately it can be estimated from the *average detection threshold* [8]:

$$\text{ADT}(c) = E\{\beta(z)y\} = \int_0^\infty \int_0^\infty \beta(z)y f_{Z,Y}(z,y) dz dy. \quad (13)$$

The *SNR loss* (SNRL) with respect to the clairvoyant detector is defined as

$$\text{SNRL}(c) = \frac{\text{ADT}(c)}{\gamma_c}, \quad (14)$$

where  $\gamma_c$  is the detection threshold found by solving

$$\hat{P}_{fa} = \int_{\gamma_c}^\infty f_X(x) dx, \quad (15)$$

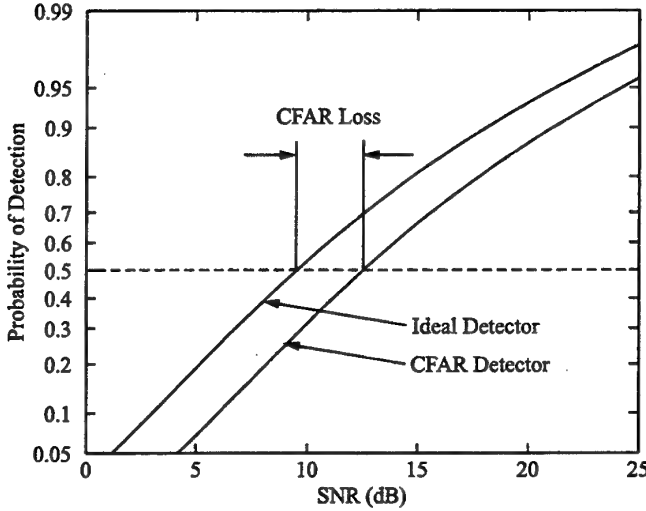


Figure 5: Depiction of the SNR loss between an ideal processor and a CFAR detection processor. SNR loss is commonly defined as the difference in SNR between the ROC curves for a specified probability of detection, which in this case is 0.5.

and  $f_X(x)$  is the gamma PDF as defined in Eq. (2). The SNR loss with respect to the OS-CFAR detector is

$$\text{SNRL}(c) = \frac{\text{ADT}(c)}{\beta_0 E\{Y|c\}}, \quad (16)$$

where  $\beta_0$  is the multiplier for the OS-CFAR detector [5]. Both the clairvoyant and OS-CFAR detectors assume the value of the shape parameter is known. Thus, the SNRL varies with respect to the value of the shape parameter, so an overall measure of SNR loss is the *average SNR loss* that is defined to be

$$\text{ASNRL} = \frac{1}{c_{max} - c_{min}} \int_{c_{min}}^{c_{max}} \text{SNRL}(c) dc \quad (17)$$

where  $[c_{min}, c_{max}]$  is the specified shape parameter design range for the PIFAR detection processor.

Figures 6 through 9 display the ASNRL for the processors whose non-linearities are approximated by the polynomials whose coefficients are listed in Appendix A. These averages were computed over the interval  $5 < c < 30$  and are displayed as a function of the number of data cells,  $N$ . Note that with respect to the clairvoyant detector the ASNRL is generally below 1 dB, which is generally considered to be an acceptable loss. Also note that as the number of cells increases, the SNRL decreases. This is as expected, because increasing the number of data cells increases the quality of data presented to the detection processor leading to an improved effective estimate of the shape parameter.

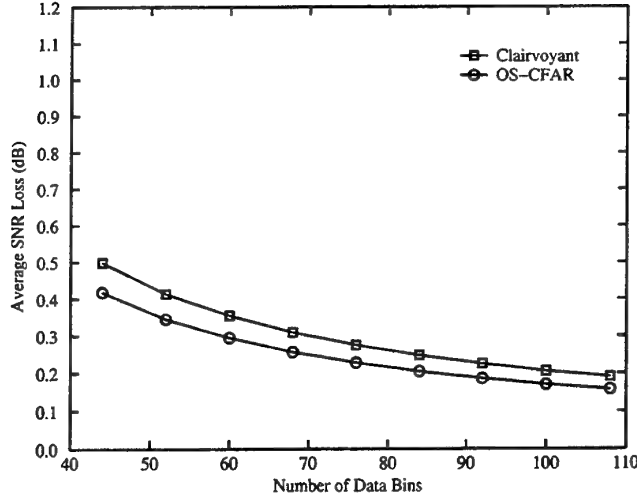


Figure 6: The average SNR loss (ASNRL) in dB as a function of the number of data cells ( $N$ ) for PIFAR processors with a design probability of false alarm of  $10^{-3}$ . For these processors,  $N = 4K$ ,  $I = K$  and  $j = 3K$  where  $K$  is an integer.

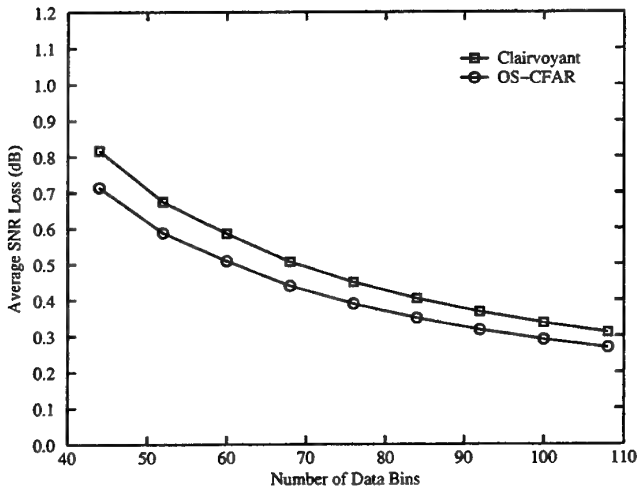


Figure 7: The average SNR loss (ASNRL) in dB as a function of the number of data cells ( $N$ ) for PIFAR processors with a design probability of false alarm of  $10^{-4}$ . For these processors,  $N = 4K$ ,  $I = K$  and  $j = 3K$  where  $K$  is an integer.

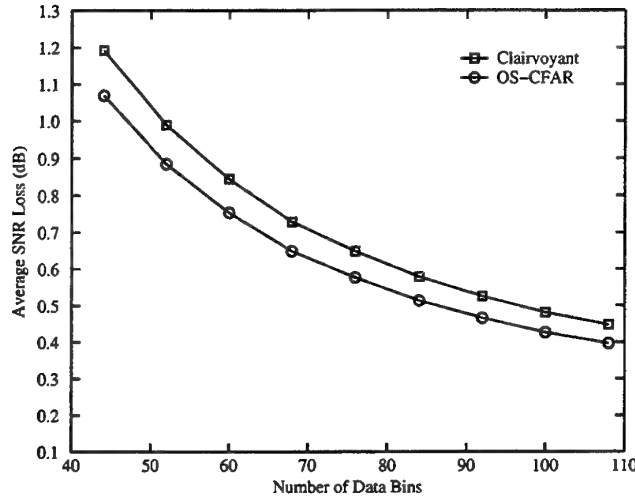


Figure 8: The average SNR loss (ASNRL) in dB as a function of the number of data cells ( $N$ ) for PIFAR processors with a design probability of false alarm of  $10^{-5}$ . For these processors,  $N = 4K$ ,  $I = K$  and  $j = 3K$  where  $K$  is an integer.

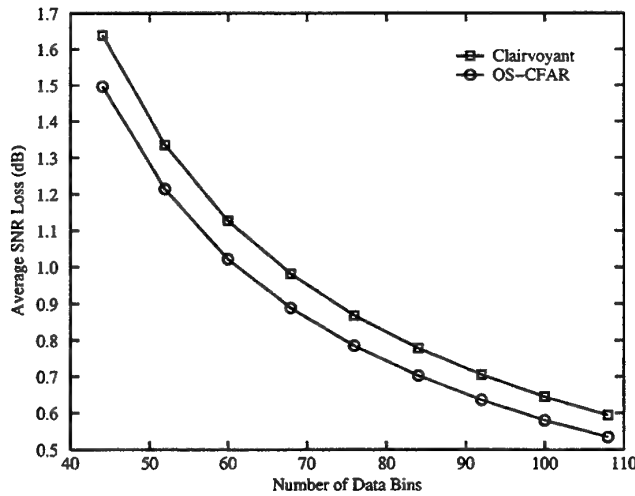


Figure 9: The average SNR loss (ASNRL) in dB as a function of the number of data cells ( $N$ ) for PIFAR processors with a design probability of false alarm of  $10^{-6}$ . For these processors,  $N = 4K$ ,  $I = K$  and  $j = 3K$  where  $K$  is an integer.

## 7 Conclusion

This report documents a detection processor that may be used in an active, incoherent sonar system provided that the receiver output follows a gamma PDF whose shape parameter is between 5 and 30. The numerical algorithm used for designing PIFAR detection processors described in this report may certainly be applied to design PIFAR detection processors for other ranges of the shape parameters. If the shape parameter is always expected to be large ( $c > 40$ ) then it is probably reasonable to assume that the receiver output follows a Gaussian PDF. In this case it is more appropriate to use a detection processor that is specifically designed for such a statistical model. Furthermore, it is possible that PIFAR detection processors can be designed for other statistical models, such as the K-type PDF, that are commonly encountered in active systems in which sonar returns are coherently processed.

## References

1. Weber, P., Haykin. S., "Order Statistic CFAR Processing Two-Parameter Distributions with Variable Skewness," *IEEE Transactions on Aerospace and Electronic Systems*, Vol. AES-21, No. 6, November 1985, 819-821.
2. Levanon, N., Shor, M., "Order Statistic CFAR for Weibull background," *IEE Proceedings*, Vol. 137, Pt. F, No. 3, June 1990, 157-162.
3. H. M. Finn and R. S. Johnson, "Adaptive Detection Mode with Threshold Control as a Function of Spatially Sampled Clutter-Level Estimates," *RCA Review*, **29**, No. 3, 414 (Sept. 1968).
4. Ritcey, J. A., "Performance Analysis of the Censored Mean-Level Detector," *IEEE Transactions on Aerospace and Electronic Systems*, Vol. AES-22, No. 6, July 1986, 443-453.
5. Rohling, H., "Radar CFAR Thresholding in Clutter and Multiple Target Situations," *IEEE Transactions on Aerospace and Electronic Systems*, Vol. AES-19, No. 4, July 1983, 608-621.
6. Shor, M., Levanon, N., "Performance of Order Statistics CFAR," *IEEE Transactions on Aerospace and Electronic Systems*, Vol. 27, No. 2, March 1991, 214-224.
7. M. Fisz, *Probability Theory and Mathematical Statistics*, John Wiley and Sons, New York, 1963.
8. Rifkin, R., "Analysis of CFAR Performance in Weibull Clutter," *IEEE Transactions on Aerospace and Electronic Systems*, Vol. 30, No. 2, April 1994, 315-329.

## Appendix A: Polynomial Approximations to PIFAR Detector Non-Linearities

The following four tables list the coefficients of polynomial approximations to a PIFAR detection processor non-linearity,  $\beta(\cdot)$ . This included the polynomial coefficients ( $b_8, b_7, \dots, b_0$ ), as well as the their argument limits ( $z_L$  and  $z_H$ ) and bounds ( $b_L$  and  $b_H$ ). The approximations are evaluated as follows:

$$\beta(Z) \approx \begin{cases} b_L & \text{for } Z \leq z_L, \\ \sum_{l=0}^8 b_l Z^l & \text{for } z_L < Z < z_H, \\ b_H & \text{for } z_H \leq Z. \end{cases} \quad (\text{A1})$$

where

$$Z = \ln(Y_j/Y_i) \quad (\text{A2})$$

and  $Y_i$  and  $Y_j$  are respectively the  $i$ -th and  $j$ -th rank ordered values for the data cell values with  $Y_i < Y_j$ .

PIFAR detection processor non-linearities can be designed for false alarm probabilities that are between those listed in the tables. Let  $\hat{P}_{fa,1} = 10^{-n-1} < 10^{-n} = \hat{P}_{fa,2}$  for some choice of integers  $n, N, i$  and  $j$ . The non-linearity

$$\beta(z) = w\beta_1(z) + (1-w)\beta_2(z), \quad (\text{A3})$$

with  $0 \leq w \leq 1$ , yields a PIFAR detection processor whose design probability of false alarm,  $\hat{P}_{fa}$ , is given by

$$\log_{10}(\hat{P}_{fa}) = w \log_{10}(\hat{P}_{fa,1}) + (1-w) \log_{10}(\hat{P}_{fa,2}) \quad (\text{A4})$$

where  $\beta_1(z)$  and  $\beta_2(z)$  are the non-linearities for PIFAR detection processors with design false alarm probabilities  $\hat{P}_{fa,1}$  and  $\hat{P}_{fa,2}$ . The error between the actual and design false alarm probabilities of this “interpolated” detection processor will not be any greater than the errors of the original detection processors.

Table A1: Argument limits and bounds for the eighth-order polynomial approximations to PIFAR detection processor non-linearities, where  $N$  is the number of data cells and  $i$  and  $j$  are the rank orders.

$\hat{P}_{fa}$	$N$	$i$	$j$	$b_L$	$b_H$	$z_L$	$z_H$
$10^{-3}$	44	11	33	1.39454732	3.86121982	0.16866630	1.02227487
$10^{-3}$	52	13	39	1.40095829	3.79427733	0.17631236	1.02220431
$10^{-3}$	60	15	45	1.40478272	3.75969079	0.18359136	1.02367210
$10^{-3}$	68	17	51	1.40797416	3.72850078	0.18826883	1.02431758
$10^{-3}$	76	19	57	1.41048830	3.70234778	0.19081198	1.02399012
$10^{-3}$	84	21	63	1.41207546	3.68442101	0.19373351	1.02486708
$10^{-3}$	92	23	69	1.41318252	3.66873238	0.19583288	1.02573532
$10^{-3}$	100	25	75	1.41370261	3.65397254	0.19680136	1.02641047
$10^{-3}$	108	27	81	1.41231875	3.65019669	0.19757824	1.02717994
$10^{-4}$	44	11	33	1.49474675	4.98615043	0.14821107	1.02283892
$10^{-4}$	52	13	39	1.50453487	4.88953094	0.15877295	1.02269018
$10^{-4}$	60	15	45	1.50818873	4.85274491	0.16840863	1.02422700
$10^{-4}$	68	17	51	1.51345454	4.80826047	0.17508106	1.02452170
$10^{-4}$	76	19	57	1.51778182	4.77057835	0.18021780	1.02370808
$10^{-4}$	84	21	63	1.52131394	4.74627490	0.18378082	1.02419922
$10^{-4}$	92	23	69	1.52433689	4.72484829	0.18717261	1.02484775
$10^{-4}$	100	25	75	1.52679106	4.70398248	0.18879006	1.02535105
$10^{-4}$	108	27	81	1.52881390	4.68589780	0.19051139	1.02584550
$10^{-5}$	44	11	33	1.57608395	6.15243956	0.13906782	1.02520394
$10^{-5}$	52	13	39	1.58562470	6.03313677	0.14879656	1.02465305
$10^{-5}$	60	15	45	1.59448884	5.96348300	0.15695205	1.02601756
$10^{-5}$	68	17	51	1.60638648	5.87171391	0.16386281	1.02524225
$10^{-5}$	76	19	57	1.61031725	5.83370751	0.16954886	1.02380844
$10^{-5}$	84	21	63	1.61880805	5.78000769	0.17409797	1.02397569
$10^{-5}$	92	23	69	1.62344193	5.75197894	0.17878542	1.02421199
$10^{-5}$	100	25	75	1.62711023	5.72514742	0.18093757	1.02438771
$10^{-5}$	108	27	81	1.62540493	5.73577227	0.18240055	1.02404116
$10^{-6}$	44	11	33	1.65164957	7.41817475	0.12778637	1.02302368
$10^{-6}$	52	13	39	1.67014117	7.18032974	0.13872140	1.02483661
$10^{-6}$	60	15	45	1.68358192	7.04763233	0.14808194	1.02726286
$10^{-6}$	68	17	51	1.68975462	6.96177664	0.15498250	1.02730956
$10^{-6}$	76	19	57	1.69685879	6.89207546	0.16068364	1.02519294
$10^{-6}$	84	21	63	1.70271217	6.84816946	0.16548193	1.02472627
$10^{-6}$	92	23	69	1.70834514	6.81013699	0.17002270	1.02444524
$10^{-6}$	100	25	75	1.71316599	6.77508826	0.17332235	1.02413375
$10^{-6}$	108	27	81	1.71778859	6.74443454	0.17648727	1.02377344

Table A2: Coefficients  $b_5$  through  $b_8$  for the eighth-order polynomial approximations to PIFAR detection processor non-linearities, where  $N$  is the number of data cells and  $i$  and  $j$  are the rank orders.

$\hat{P}_{fa}$	$N$	$i$	$j$	$b_8$	$b_7$	$b_6$	$b_5$
$10^{-3}$	44	11	33	-183.91514677	949.92372623	-2064.45869504	2460.19952451
$10^{-3}$	52	13	39	-135.46790789	740.71790896	-1686.94077877	2085.49411736
$10^{-3}$	60	15	45	-122.65906772	731.78447496	-1789.29683925	2349.13036033
$10^{-3}$	68	17	51	-49.11856651	395.30211642	-1151.10691467	1698.63469976
$10^{-3}$	76	19	57	92.73980786	-297.15516773	273.09937515	91.49289604
$10^{-3}$	84	21	63	166.67209015	-658.21012531	1011.40055232	-730.37228035
$10^{-3}$	92	23	69	227.59671548	-968.48037201	1673.46729205	-1500.73087701
$10^{-3}$	100	25	75	285.60355634	-1277.96379676	2365.08523288	-2344.41263832
$10^{-3}$	108	27	81	322.39054325	-1470.76942863	2784.28948254	-2836.77943231
$10^{-4}$	44	11	33	-376.01304082	1791.63004715	-3575.98701302	3888.85304522
$10^{-4}$	52	13	39	-410.57224268	2004.44207351	-4094.23511184	4546.44869008
$10^{-4}$	60	15	45	-493.87466150	2522.58031973	-5401.97290687	6309.57454635
$10^{-4}$	68	17	51	-419.66065932	2241.14127632	-5000.93959143	6069.41970903
$10^{-4}$	76	19	57	-259.00754858	1524.39834607	-3678.16012406	4762.52382852
$10^{-4}$	84	21	63	-10.55600443	358.87126120	-1385.60834319	2303.65898419
$10^{-4}$	92	23	69	187.83974531	-587.70710612	506.51409264	243.82608576
$10^{-4}$	100	25	75	409.46960084	-1687.31102183	2803.10525355	-2384.43324889
$10^{-4}$	108	27	81	563.10842177	-2463.28535712	4449.41442149	-4294.01683559
$10^{-5}$	44	11	33	-1095.89873609	5167.48955684	-10245.79807493	11119.38595813
$10^{-5}$	52	13	39	-1146.78025800	5454.36042841	-10898.09184510	11909.93947152
$10^{-5}$	60	15	45	-1131.60402686	5484.69676199	-11157.23176359	12399.75177906
$10^{-5}$	68	17	51	-1032.68459893	5131.38566528	-10692.32803417	12150.49759723
$10^{-5}$	76	19	57	-884.90462837	4549.73148801	-9791.72029575	11477.25848417
$10^{-5}$	84	21	63	-494.68347457	2762.21218960	-6367.32799391	7906.58905873
$10^{-5}$	92	23	69	-225.01018766	1547.55182133	-4096.45549789	5623.51976470
$10^{-5}$	100	25	75	162.30474529	-302.32857071	-382.59982011	1545.03206306
$10^{-5}$	108	27	81	559.44327760	-2161.19178803	3272.35491913	-2380.59724226
$10^{-6}$	44	11	33	-531.86557821	2734.17278842	-5964.57543081	7200.11347411
$10^{-6}$	52	13	39	-1258.66712834	5902.11086601	-11626.26358086	12542.97551529
$10^{-6}$	60	15	45	-1680.09633139	7944.28023825	-15745.22669074	17023.35148612
$10^{-6}$	68	17	51	-1773.66953309	8513.22391107	-17128.59457528	18796.23479738
$10^{-6}$	76	19	57	-1690.59650616	8270.86626223	-16955.76142102	18948.29898314
$10^{-6}$	84	21	63	-1418.00579711	7141.89553376	-15048.04277044	17256.12162002
$10^{-6}$	92	23	69	-1089.77314080	5732.52262691	-12558.13991222	14917.80373211
$10^{-6}$	100	25	75	-658.62221814	3776.00301163	-8852.54782323	11110.17263411
$10^{-6}$	108	27	81	-204.16377317	1681.97867321	-4818.91920654	6887.76003722

Table A3: Coefficients  $b_1$  through  $b_4$  for the eighth-order polynomial approximations to PIFAR detection processor non-linearities, where  $N$  is the number of data cells and  $i$  and  $j$  are the rank orders.

$\hat{P}_{fa}$	$N$	$i$	$j$	$b_4$	$b_3$	$b_2$	$b_1$
$10^{-3}$	44	11	33	-1752.75783591	759.51481746	-193.27948489	29.11329183
$10^{-3}$	52	13	39	-1526.40760660	674.16016589	-174.13940117	26.75321256
$10^{-3}$	60	15	45	-1812.38621964	840.17653174	-227.62948246	35.60643898
$10^{-3}$	68	17	51	-1426.33965498	705.59089484	-201.40483667	33.05807238
$10^{-3}$	76	19	57	-341.17298712	257.96091684	-91.56315038	18.37795237
$10^{-3}$	84	21	63	201.00554157	42.03461711	-41.15259358	12.06266741
$10^{-3}$	92	23	69	733.71357160	-181.33110577	14.11274485	4.67063422
$10^{-3}$	100	25	75	1346.77869619	-452.44499941	85.21798811	-5.45599732
$10^{-3}$	108	27	81	1687.13179995	-593.62404877	119.44409729	-9.91396782
$10^{-4}$	44	11	33	-2503.62122268	964.24387424	-212.24733163	28.24673098
$10^{-4}$	52	13	39	-2982.70245149	1172.45107165	-265.94577928	35.55251410
$10^{-4}$	60	15	45	-4377.18550994	1835.91540436	-450.76265723	62.75940973
$10^{-4}$	68	17	51	-4365.65497368	1896.52809799	-482.57207911	69.21762071
$10^{-4}$	76	19	57	-3619.25448293	1649.54262448	-438.20276943	65.53785803
$10^{-4}$	84	21	63	-2053.50464960	1046.47734744	-301.78112074	48.97785195
$10^{-4}$	92	23	69	-724.50841029	529.07004642	-183.84673434	34.61990403
$10^{-4}$	100	25	75	1072.04974171	-219.49377515	1.22111631	9.80544259
$10^{-4}$	108	27	81	2391.89074129	-774.15884891	139.17417506	-8.75980089
$10^{-5}$	44	11	33	-7185.02915042	2800.69278004	-632.76383943	80.73185499
$10^{-5}$	52	13	39	-7755.36533342	3058.96047700	-705.06755244	91.42053636
$10^{-5}$	60	15	45	-8204.51933241	3290.91251528	-774.02596319	101.99627294
$10^{-5}$	68	17	51	-8197.71073929	3342.57990019	-797.84949685	106.30011241
$10^{-5}$	76	19	57	-7982.33849056	3356.52380054	-827.32779266	113.52029754
$10^{-5}$	84	21	63	-5771.86835527	2527.03117587	-644.08224981	91.76443942
$10^{-5}$	92	23	69	-4435.91176956	2068.25503509	-556.01755472	83.41164200
$10^{-5}$	100	25	75	-1766.08339319	1005.52239521	-305.71916599	51.51560267
$10^{-5}$	108	27	81	739.27277277	38.81946223	-86.59263107	24.82456041
$10^{-6}$	44	11	33	-5209.30165390	2258.34386769	-553.36458101	76.38759215
$10^{-6}$	52	13	39	-8079.55413482	3153.11079932	-715.49522400	92.17956839
$10^{-6}$	60	15	45	-10935.78816776	4245.43019478	-962.22604401	122.05783080
$10^{-6}$	68	17	51	-12254.48606915	4833.00633441	-1116.11617402	143.32446012
$10^{-6}$	76	19	57	-12573.30667397	5046.38651258	-1187.04036191	154.75419784
$10^{-6}$	84	21	63	-11732.80684593	4819.87416267	-1159.82887412	154.51432626
$10^{-6}$	92	23	69	-10475.71004332	4434.36310992	-1097.71952454	150.32561575
$10^{-6}$	100	25	75	-8165.77099428	3592.24814417	-918.87984855	130.12417840
$10^{-6}$	108	27	81	-5551.52214064	2617.41972818	-706.45292716	105.44332593

Table A4: Coefficient  $b_0$  (additive constant) for the eighth-order polynomial approximations to PIFAR detection processor non-linearities, where  $N$  is the number of data cells and  $i$  and  $j$  are the rank orders.

$\hat{P}_{fa}$	$N$	$i$	$j$	$b_0$
$10^{-3}$	44	11	33	-0.53510906
$10^{-3}$	52	13	39	-0.43104319
$10^{-3}$	60	15	45	-1.02633239
$10^{-3}$	68	17	51	-0.94733160
$10^{-3}$	76	19	57	-0.13611938
$10^{-3}$	84	21	63	0.18315889
$10^{-3}$	92	23	69	0.58807933
$10^{-3}$	100	25	75	1.18395235
$10^{-3}$	108	27	81	1.42091253
$10^{-4}$	44	11	33	-0.20353823
$10^{-4}$	52	13	39	-0.63137657
$10^{-4}$	60	15	45	-2.26562180
$10^{-4}$	68	17	51	-2.75439162
$10^{-4}$	76	19	57	-2.68696206
$10^{-4}$	84	21	63	-1.87238485
$10^{-4}$	92	23	69	-1.16815499
$10^{-4}$	100	25	75	0.20586533
$10^{-4}$	108	27	81	1.23485859
$10^{-5}$	44	11	33	-2.76805851
$10^{-5}$	52	13	39	-3.44173854
$10^{-5}$	60	15	45	-4.11843726
$10^{-5}$	68	17	51	-4.42999976
$10^{-5}$	76	19	57	-5.01031179
$10^{-5}$	84	21	63	-3.96760849
$10^{-5}$	92	23	69	-3.70623457
$10^{-5}$	100	25	75	-2.03313535
$10^{-5}$	108	27	81	-0.70158373
$10^{-6}$	44	11	33	-2.61777238
$10^{-6}$	52	13	39	-3.34080968
$10^{-6}$	60	15	45	-4.87639251
$10^{-6}$	68	17	51	-6.09670987
$10^{-6}$	76	19	57	-6.83541254
$10^{-6}$	84	21	63	-7.00473622
$10^{-6}$	92	23	69	-6.99746448
$10^{-6}$	100	25	75	-6.08620722
$10^{-6}$	108	27	81	-4.93214678

## DISTRIBUTION LIST

### A Parameter-Insensitive False Alarm Rate Detection Processor

David M. Drumheller and Henry Lew

	Number of Copies
<b>DEFENCE ORGANISATION</b>	
<b>Task Sponsor</b>	
Director General Maritime Development	1
SOUWW, DGMD	1
<b>S&amp;T Program</b>	
Chief Defence Scientist	1
FAS Science Policy	1
AS Science Corporate Management	1
Director General Science Policy Development	1
Counsellor, Defence Science, London	Doc Data Sht
Counsellor, Defence Science, Washington	Doc Data Sht
Scientific Adviser to MRDC, Thailand	Doc Data Sht
Scientific Adviser Policy and Command	1
Navy Scientific Adviser	1
Scientific Adviser, Army	Doc Data Sht
Air Force Scientific Adviser	1
Director Trials	1
<b>Aeronautical and Maritime Research Laboratory</b>	
Director, Aeronautical and Maritime Research Laboratory	1
Chief, Maritime Operations Division	1
Research Leader Maritime Sensor Systems	1
Research Leader Submarine Operations	1
Research Leader Mine Warfare	1
Head Sonar Processing and Systems	1
D. Drumheller, MOD Salisbury	1
R. Ellem, MOD Salisbury	1
L. Kelly, MOD Salisbury	1
A. Larsson, MOD Salisbury	1
H. Lew, MOD Salisbury	2
S. Lourey, MOD Salisbury	1
D. Solomon, MOD Salisbury	1
D. Sweet, MOD Salisbury	1

M. Swift, MOD Salisbury	1
S. Taylor, MOD Salisbury	1
J. Wang, MOD Salisbury	1
<b>DSTO Libraries and Archives</b>	
Library Fishermans Bend	1
Library Maribyrnong	Doc Data Sht
Library Salisbury	1
Australian Archives	1
Library, MOD, HMAS Stirling	1
Library, MOD, Pyrmont	Doc Data Sht
US Defense Technical Information Center	2
UK Defence Research Information Centre	2
Canada Defence Scientific Information Service	1
NZ Defence Information Centre	1
National Library of Australia	1
<b>Capability Systems Staff</b>	
DDSMWD R1-3-C013	Doc Data Sht
<b>Knowledge Staff</b>	
Director General Command, Control, Communications and Computers (DGC4)	Doc Data Sht
Director General Intelligence, Surveillance, Reconnaissance and Electronic Warfare (DGISREW)R1-3-A142 Canberra ACT 2600	Doc Data Sht
Director General Defence Knowledge Improvement Team (DGDKNIT)R1-5-A165 Canberra ACT 2600	Doc Data Sht
<b>Navy</b>	
COM AUS NAV SURF GRP - Attn: Cmdr B. Chandler	1
SO(Science), COMAUSNAVSURFGRP, Bldg 95, Garden Island, Pyrmont NSW 2009	Doc Data Sht
<b>Intelligence Program</b>	
DGSTA Defence Intelligence Organisation	1
Manager, Information Centre, Defence Intelligence Organisation	1
<b>Acquisition Program</b>	
ASSTASS Project Director	1
<b>Corporate Support Program</b>	
Library Manager, DLS-Canberra	1

**UNIVERSITIES AND COLLEGES**

Australian Defence Force Academy Library	1
Head of Aerospace and Mechanical Engineering, ADFA	1
Deakin University Library, Serials Section (M List)	1
Hargrave Library, Monash University	Doc Data Sht
Librarian, Flinders University	1

**OTHER ORGANISATIONS**

NASA (Canberra)	1
AusInfo	1

**ABSTRACTING AND INFORMATION ORGANISATIONS**

Engineering Societies Library, US	1
Library, Chemical Abstracts Reference Service	1
Engineering Societies Library, US	1
Materials Information, Cambridge Science Abstracts, US	1
Documents Librarian, The Center for Research Libraries, US	1

**INFORMATION EXCHANGE AGREEMENT PARTNERS**

Acquisitions Unit, Science Reference and Information Service, UK	1
Library – Exchange Desk, National Institute of Standards and Technology, US	1

**SPARES**

DSTO Salisbury Research Library	5
---------------------------------	---

**Total number of copies:** 60

<b>DEFENCE SCIENCE AND TECHNOLOGY ORGANISATION DOCUMENT CONTROL DATA</b>		1. CAVEAT/PRIVACY MARKING								
<b>2. TITLE</b> A Parameter-Insensitive False Alarm Rate Detection Processor		<b>3. SECURITY CLASSIFICATION</b> Document (U) Title (U) Abstract (U)								
<b>4. AUTHORS</b> David M. Drumheller and Henry Lew		<b>5. CORPORATE AUTHOR</b> Aeronautical and Maritime Research Laboratory 506 Lorimer St, Fishermans Bend, Victoria, Australia 3207								
<b>6a. DSTO NUMBER</b> DSTO-TR-1153	<b>6b. AR NUMBER</b> AR-011-869	<b>6c. TYPE OF REPORT</b> Technical Report	<b>7. DOCUMENT DATE</b> June, 2001							
<b>8. FILE NUMBER</b> P9505/19/250	<b>9. TASK NUMBER</b> NAV 99/027	<b>10. SPONSOR</b> DGMD	<b>11. No OF PAGES</b> 18	<b>12. No OF REFS</b> 8						
<b>13. URL OF ELECTRONIC VERSION</b> <a href="http://www.dsto.defence.gov.au/corporate/reports/DSTO-TR-1153.pdf">http://www.dsto.defence.gov.au/corporate/reports/DSTO-TR-1153.pdf</a>		<b>14. RELEASE AUTHORITY</b> Chief, Maritime Operations Division								
<b>15. SECONDARY RELEASE STATEMENT OF THIS DOCUMENT</b> <i>Approved For Public Release</i> <small>OVERSEAS ENQUIRIES OUTSIDE STATED LIMITATIONS SHOULD BE REFERRED THROUGH DOCUMENT EXCHANGE, PO BOX 1500, SALISBURY, SOUTH AUSTRALIA 5108</small>										
<b>16. DELIBERATE ANNOUNCEMENT</b> No Limitations										
<b>17. CITATION IN OTHER DOCUMENTS</b> No Limitations										
<b>18. DEFTEST DESCRIPTORS</b> <table> <tr> <td>Sonar detectors</td> <td>Detection processors</td> </tr> <tr> <td>Active Sonar</td> <td>False alarms</td> </tr> <tr> <td>Detection threshold</td> <td>Probability density functions</td> </tr> </table>					Sonar detectors	Detection processors	Active Sonar	False alarms	Detection threshold	Probability density functions
Sonar detectors	Detection processors									
Active Sonar	False alarms									
Detection threshold	Probability density functions									
<b>19. ABSTRACT</b> <p>In active sonar systems, detection is the process of deciding if a target echo is present in a return. This is often accomplished by an operator who examines the sonar receiver output and decides if any portion of it is larger than the expected response due to reverberation. Detection may also be accomplished automatically using a processor that sets a threshold based on a sampling of the receiver output. In this report, a detection processor developed under the task NAV 99/027 is presented for use in active sonar systems that process returns incoherently. The statistics of the receiver output of such a system follows the two-parameter gamma probability density function (PDF). Consequently, the detection processor computes the detection threshold as a non-linear function of the ratio of two ranked values of the receiver output. The result is a detection processor that exhibits a false alarm probability that is bounded within ten percent of a design value regardless of the values of the gamma PDF parameters.</p>										

